Nuclear spin selective alignment of ethylene and analogues

Thomas Grohmann and Monika Leibscher

Citation: The Journal of Chemical Physics **134**, 204316 (2011); doi: 10.1063/1.3595133
View online: http://dx.doi.org/10.1063/1.3595133
View Table of Contents: http://scitation.aip.org/content/aip/journal/jcp/134/20?ver=pdfcov
Published by the AIP Publishing

Nuclear spin selective alignment of ethylene and analogues

Thomas Grohmann and Monika Leibscher[a)]
Institut für Chemie und Biochemie, Freie Universität Berlin, Takustr. 3, 14195 Berlin, Germany

(Received 19 January 2011; accepted 7 May 2011; published online 31 May 2011)

We investigate the alignment of ethylene and of some of its analogues via short, non-resonant laser pulses and show that it depends crucially on the nuclear spin of the molecules. We calculate the time-dependent alignment factors of the four nuclear spin isomers of ethylene and analyze them by comparison with the symmetric top molecule allene. Moreover, we explore how the nuclear spin selective alignment depends on the asymmetry of the molecules and on the intensity of the laser pulse. As an application, we discuss how nuclear spin selective alignment could be applied in order to separate different isotopomers of ethylene. © *2011 American Institute of Physics*. [doi:10.1063/1.3595133]

I. INTRODUCTION

The connection of nuclear spin and molecular properties is one of the oldest stories in quantum mechanics. First predicted by Heisenberg[1] and Hund[2] to explain the "anomalous" intensity alternating in Raman spectra, the existence of nuclear isomers has been proven by Bonhoeffer and Harteck,[3] who verified experimentally that hydrogen has two nuclear spin modifications, para- and ortho-hydrogen, having different specific heats. However, specific heat is not the only molecular property which is substantially different for distinct nuclear spin isomers. It is well known that they can be distinguished by their rotational spectra, since different nuclear spin isomers belong to rotational states of different symmetry.[4] As a consequence, rotational dynamics will also depend on the nuclear spin of the molecules.

Rotational dynamics, especially the alignment of molecules induced by strong, non-resonant laser pulses is momentarily intensively studied[5–17] (for a review see Refs. 18 and 19); many possible applications are explored, among them the separation of stereoisomers,[20] the control of molecular scattering,[21,22] the determination of ionization probabilities,[23] orbital imaging and high harmonics generation,[24–26] and x-ray scattering.[27] However, in most investigations carried out so far the role of nuclear spin on such processes is less studied although it has been shown for diatomic molecules[28–30] and for water[31] that different nuclear spin isomers show different rotational dynamics. For homo-nuclear diatomic molecules, it has been observed that the transient alignment after interaction with a short laser pulse depends crucially on the nuclear spin: at specific times, one nuclear spin isomer is aligned along the polarization direction of the laser pulse, while the other isomer is aligned perpendicular to it. It has been suggested to use sequences of laser pulses to selectively manipulate the rotational dynamics of nuclear spin isomers of diatomic molecules.[28] Also polyatomic molecules can occur in form of nuclear spin isomers.[32,33] With the exception of water,[31] the nuclear spin selective alignment of non-linear molecules has - as far as we know - not be investigated. However, it becomes especially interesting for molecules, which have more than two nuclear spin modifications, for example allene or ethylene (see Fig. 1). Here, we investigate the rotational dynamics, in particular the laser induced alignment of the nuclear spin isomers of molecules with different degree of asymmetry. We consider the symmetric top molecule allene and the asymmetric top molecule ethylene and analogues, shown in Fig. 1. Therefore, we discuss in Sec. II how nuclear spin isomers of (rigid) molecules can be found and identify the nuclear spin isomers for these molecules. Afterwards, we will present the theory of non-adiabatic, non-resonant alignment, before we discuss in Sec. IV our results.

II. NUCLEAR SPIN ISOMERS AND ROTATIONAL SPECTRA

Molecules containing two or more identical nuclei with non-zero spin occur in isomeric forms which are called nuclear spin modifications or nuclear spin isomers. They are a consequence of the symmetrization postulate, which only allows distinct symmetry combinations of rovibronic and nuclear spin states. If rovibronic states of different symmetries correspond to different energies, nuclear spin isomers of rigid molecules can—as we illustrate below—distinguished by their rotational spectra. Their identification relies on the assumption that the interactions between nuclear spins and the spatial molecular degrees of freedom is so small that nuclear spin isomers can be regarded as stable species especially for the time-scales considered here, which are 100 ps or less.

The symmetrization postulate states that any molecular wave function Φ^{mol} representing a physical state must change its sign if two fermionic nuclei are exchanged and remains unchanged upon the exchange of two bosonic nuclei. Thus, the molecular wave function must have a distinct symmetry under permutations of identical nuclei. The symmetry groups appropriate for classifying molecular states according to these permutations, are the permutation subgroups of molecular symmetry (MS) groups,[34] which contain all feasible permutations P of identical nuclei (note, that often the MS group is used to find the nuclear spin isomers of molecules. In Appendix A, we will discuss why this can lead to ambiguities making it

a)Electronic mail: monika.leibscher@chemie.fu-berlin.de.

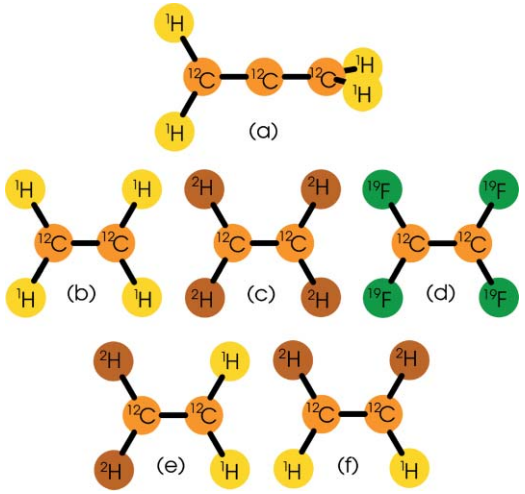

FIG. 1. The molecules we investigate in our study: (a) allene (C_3H_4), (b) ethylene (C_2H_4), (c) fully deuterated ethylene (C_2D_4), (d) tetrafluoro ethylene (C_2F_4), (e) [1,1-$^2H_2$]ethylene (1,1-$C_2H_2D_2$), and (f) (*Z*)-[1,2-$^2H_2$]ethylene ((*Z*)-1,2-$C_2H_2D_2$). All carbon nuclei are assumed to be C $\equiv^{12}$ C. We will use the same color code for the nuclei throughout this paper.

necessary to use the permutation subgroup of the MS group). Within the permutation subgroup, any molecular state Φ^{mol} must transform according to the irreducible, one-dimensional and real representation $\mathbf{\Gamma}^{\mathrm{mol}}$ having the character $\chi = -1$ for any permutation containing an odd number of transpositions of fermionic nuclei and the character $\chi = +1$ for either permutations containing an even number of transpositions of fermionic nuclei or for permutations containing an even or odd number of transpositions of bosonic nuclei.[4]

The MS-groups for the molecules shown in Fig. 1 are reported in the literature:[4] For all C_2X_4-type molecules it is the group $D_{2h}(M)$, for allene it is $D_{2d}(M)$. Both groups have the same permutation subgroup, which reads (see Fig. 2)

$$\mathrm{D}_2(\mathrm{M}) = \{E, (\mathbf{a}), (\mathbf{b}), (\mathbf{c})\} \ ; \tag{2.1}$$

the abbreviations are

$$(\mathbf{a}) = (12)(34), \tag{2.2a}$$

$$(\mathbf{b}) = (13)(24)(56), \tag{2.2b}$$

$$(\mathbf{c}) = (14)(23)(56)\,, \tag{2.2c}$$

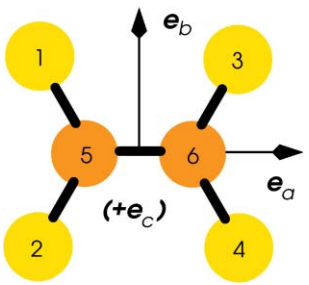

FIG. 2. Sketch of the reference structure of rigid C_2X_4-type molecules. The labeling of the nuclei and the principal axes of the moment of inertia tensor are shown as well.

TABLE I. Character table of the permutation group $D_2(M)$ defined in Eq. (2.1) together with the equivalent rotations R_i^{α}. The abbreviations for the permutations are defined in Eq. (II).

$D_2(M)$	E	(**a**)	(**b**)	(**c**)
eq. rot.	R^0	R_a^{π}	R_b^{π}	R_c^{π}
A	1	1	1	1
B_a	1	1	−1	−1
B_b	1	−1	1	−1
B_c	1	−1	−1	1

where, e.g., (12)(34) stands for the simultaneous exchange of nuclei 1 with 2 and 3 with 4. Table I reports the character table of the group Eq. (2.1) together with the equivalent rotations R_i^{π} with axis $i = a, b, c$ shown in Fig. 2. The notation R_i^{α} represents a rotation by the angle α (here $\alpha = 0$ or π) around the axis $i = a, b, c$.

For all molecules C_2X_4 the symmetrization postulate demands that Φ^{mol} has to transform according to $\mathbf{\Gamma}^{\mathrm{mol}} = \mathrm{A}$. For the partially deuterated ethylene, in particular the analogues (e) and (f) shown in Fig. 1, the permutation subgroups read

$$\mathrm{C}_2^{(\mathrm{a})}(\mathrm{M}) \equiv \{E, (\mathbf{a})\}\ , \tag{2.3a}$$

for analogue (e) and

$$\mathrm{C}_2^{(\mathrm{b})}(\mathrm{M}) \equiv \{E, (\mathbf{b})\}\ , \tag{2.3b}$$

for analogue (f). Their character tables are shown in Table II. Here, since deuteron is a boson, in both cases Φ^{mol} transforms according to $\mathbf{\Gamma}^{\mathrm{mol}} = \mathrm{B}$.

In this study, we investigate how the rotational degrees of freedom of the molecules can be manipulated via nonresonant laser pulses inducing alignment. As it has been verified experimentally, the molecules remain in their vibronic ground states during such interaction and couplings between rotations and other molecular degrees of freedom do not affect the alignment as long as one limits the observations to a few rotational periods.[14,18] It is therefore reasonable to assume that the molecular wave function Φ^{mol} can be written as

$$\Phi^{\mathrm{mol}} = \Phi^{\mathrm{el}} \cdot \Phi^{\mathrm{vib}} \cdot \Phi^{\mathrm{rot}} \cdot \Phi^{\mathrm{nu.sp}}\,, \tag{2.4}$$

where Φ^{el} denotes the electronic, Φ^{vib} the vibrational, Φ^{rot} the rotational, and $\Phi^{\mathrm{nu.sp}}$ the nuclear spin wave function. Since the vibronic ground state transforms totally symmetric in the MS group for the molecules we consider, their nuclear spin isomers are identified by different symmetry combinations of nuclear spin states and rotational states fulfilling the symmetrization postulate, i.e.,

$$\Phi^{\mathrm{rot}} \cdot \Phi^{\mathrm{nu.sp}} \sim \mathbf{\Gamma}^{\mathrm{mol}}\,. \tag{2.5}$$

The rotational states of a rigid molecule are the eigenfunctions of the Hamiltonian

$$\hat{H}^{\mathrm{rot}} = \mathfrak{A} \cdot \hat{J}_a^2 + \mathfrak{B} \cdot \hat{J}_b^2 + \mathfrak{C} \cdot \hat{J}_c^2\,, \tag{2.6}$$

with $\hat{J}_a$, $\hat{J}_b$, $\hat{J}_c$ being the dimensionless molecule-fixed angular momenta and the rotational constants $\mathfrak{A}$, $\mathfrak{B}$, $\mathfrak{C}$. Here, we consider molecules with increasing degree of asymmetry, which can be characterized by the asymmetry parameter κ,

TABLE II. Character table for the permutation group $C_2^{(a)}(M)$ (left) and $C_2^{(b)}(M)$ (right), which are defined in Eqs. (2.3a) and (2.3b), respectively, together with their equivalent rotations. The abbreviations for the permutations are defined in Eq. (2.2).

$C_2^{(a)}(M)$ eq. rot.	E R^0	(**a**) R_a^π	$C_2^{(b)}(M)$ eq. rot.	E R^0	(**b**) R_b^π
A	1	1	A	1	1
B	1	−1	B	1	−1

defined as[35]

$$\kappa \equiv \frac{2\cdot\mathfrak{B}-\mathfrak{A}-\mathfrak{C}}{\mathfrak{A}-\mathfrak{C}}\,. \tag{2.7}$$

Their rotational constants and asymmetry factors are shown in Table III: Allene is an example for a prolate symmetric top, i.e., $\kappa=-1$; ethylene is the asymmetric top most similar to a prolate symmetric rotor; and the degree of asymmetry increases when the hydrogen ^{1}H atoms are substituted with heavier nuclei. It is well known that for solving the time-independent Schrödinger equation for symmetric and asymmetric tops, the symmetric top eigenfunctions $\Phi_{J,k,m}$ are of central importance: they characterize completely all states of a symmetric top having the energy $E_{J,K}$, with $K=|k|$; for an asymmetric top molecule they serve as a basis for calculating its eigenfunctions $\Phi_{J,\tau,m}$ and eigenvalues $E_{J,\tau}$[39]. Here, we use the standard notations, i.e., J denotes the rotational quantum number; k and m are the projection quantum numbers corresponding to one molecule-fixed and space-fixed component of the total angular momentum $\hat{J}$; τ denotes the asymmetry quantum number, defined as $\tau=K_a-K_c$ with $K_a=|k_a|$ and $K_c=|k_c|$ being the absolute value of the projection quantum number corresponding to the molecule-fixed angular momenta $\hat{J}_a$ and $\hat{J}_c$. The transformation properties of the symmetric top functions $\Phi_{J,k,m}$ in the prolate (i.e., $k=k_a$) and oblate limit (i.e., $k=k_c$) under permutations is reported in the literature[4,39,40] and one can verify that the combinations of symmetric top eigenfunctions

$$\Phi^{\pm}_{J,K,m}=\frac{1}{\sqrt{2}}\left(\Phi_{J,K,m}\pm(-1)^J\Phi_{J,-K,m}\right), \tag{2.8a}$$

for $K=|k|\neq 0$ and

$$\Phi^{+}_{J,0,m}=\Phi_{J,0,m}, \tag{2.8b}$$

TABLE IV. The symmetry allowed combinations of rotational states Φ^{rot} and nuclear spin states $\Phi^{\mathrm{nu.sp}}$ for all systems considered in this study together with the weights of the nuclear spin states $g_{\Gamma^{\mathrm{nu.sp}}}$. Note, that $C_2H_2D_2$ refers to both species, (e) and (f) from Fig. 1.

C_2H_4, C_3H_4, C_2F_4			C_2D_4			$C_2H_2D_2$		
Γ^{rot}	$\Gamma^{\mathrm{nu.sp}}$	$g_{\Gamma^{\mathrm{nu.sp}}}$	Γ^{rot}	$\Gamma^{\mathrm{nu.sp}}$	$g_{\Gamma^{\mathrm{nu.sp}}}$	Γ^{rot}	$\Gamma^{\mathrm{nu.sp}}$	$g_{\Gamma^{\mathrm{nu.sp}}}$
A	A	7	A	A	27	A	B	15
B_a	B_a	3	B_a	B_a	18	B	A	21
B_b	B_b	3	B_b	B_b	18			
B_c	B_c	3	B_c	B_c	18			

for $K=0$ provide a basis for the irreducible representations for all permutation groups considered here. Note, that these functions are a modification of the conventional Wang states.[41] They transform in $D_2(M)$ according to

$$\Phi^{+}_{J,K,m}\sim\begin{cases}\mathrm{A}, & (K_a \text{ even}, K_c \text{ even})\\ \mathrm{B_b}, & (K_a \text{ odd}, K_c \text{ odd})\end{cases}, \tag{2.9a}$$

$$\Phi^{-}_{J,K,m}\sim\begin{cases}\mathrm{B_a}, & (K_a \text{ even}, K_c \text{ odd})\\ \mathrm{B_c}, & (K_a \text{ odd}, K_c \text{ even})\end{cases}. \tag{2.9b}$$

The rotational eigenfunctions have to be combined with nuclear spin functions $\Phi^{\mathrm{nu.sp}}$ with proper symmetry so that the symmetrization postulate is fulfilled. Since ^{12}C has zero nuclear spin and the nuclear spin of ^{1}H and ^{19}F is 1/2, ethylene and tetrafluoro ethylene have $2^4=16$ spin states in total; for analogue (c) from Fig. 1 there are $3^4=81$ spin states, since the nuclear spin of ^{2}H is 1; and for the analogues (e) and (f) $2^2\cdot 3^2=36$ nuclear spin states exist. Table IV shows all symmetry allowed combinations of Φ^{rot} and $\Phi^{\mathrm{nu.sp}}$ together with the statistical weights of the nuclear spin states $g_{\Gamma^{\mathrm{nu.sp}}}$.[4,32] For example, for the species with $D_2(M)$ permutational symmetry $\Gamma^{\mathrm{mol}}=\mathrm{A}$. Thus Φ^{rot} and $\Phi^{\mathrm{nu.sp}}$ have to transform according to the same irreducible representation $\Gamma=\mathrm{A}, \mathrm{B_a}, \mathrm{B_b}, \mathrm{B_c}$. In the following, we denote the nuclear spin isomers by $\Gamma^{\mathrm{rot}}[\Gamma^{\mathrm{nu.sp}}]$. Allene, ethylene, fully deuterated ethylene and tetrafluoro ethylene have four nuclear spin isomers, the partially deuterated species have two nuclear spin modifications.

TABLE III. Rotational constants (in 10^{-23}J) and the irreducible components of the dipole polarizability (in 10^{-42}Cm^2/V) for the molecules subject of this study. For ethylene, its deuterated analogues and tetrafluoro ethylene, we used values from literature (Refs. 36 and 37); for allene, we performed quantum chemistry on CCSD(T) level of theory with an augmented correlation-consistent triple zeta basis, using the package GAUSSIAN 03 (Ref. 38). Here, we use the equilibrium structure to calculate the rotation constants.

	C_3H_4	C_2H_4	(Z)-1,2-$C_2H_2D_2$	1,1-$C_2H_2D_2$	C_2D_4	C_2F_4
$\mathfrak{A}$	9.605	9.718	7.446	6.482	4.863	0.364
$\mathfrak{B}$	0.584	1.984	1.679	1.786	1.455	0.213
$\mathfrak{C}$	0.584	1.647	1.370	1.400	1.120	0.134
κ	−1	−0.917	−0.898	−0.848	−0.821	−0.312
$\alpha^{2,0}$	83.989	30.053	30.917	30.917	29.982	32.735
$\alpha^{2,2}$	0	6.339	4.947	4.947	3.842	13.442

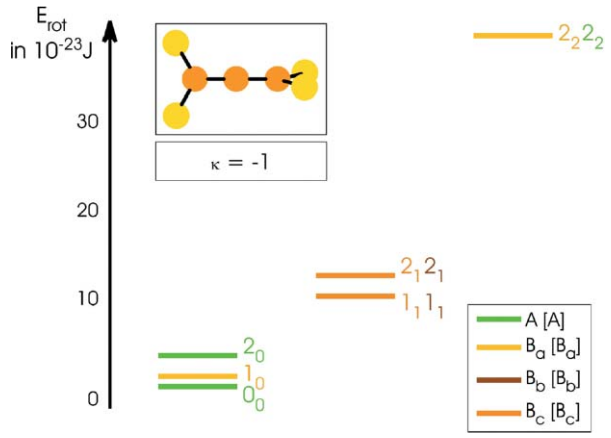

FIG. 3. Rotational spectrum of allene for $J = 0, 1, 2$. The states are labeled according to J_{K_a}.

The rotational spectrum of allene, i.e., the representation of the eigenvalues

$$E_{J,K_a} = \mathfrak{B}J(J+1) + (\mathfrak{A} - \mathfrak{B})K_a^2 \,, \tag{2.10}$$

for all nuclear spin isomers is shown in Fig. 3. The rotational states are labeled with J_{K_a}. The nuclear spin isomers can be divided by their rotational energies into two groups: the isomers A[A] and $B_a[B_a]$ (first and third column in Fig. 3) with the quantum number K_a being even and the isomers $B_b[B_b]$ and $B_c[B_c]$ (second column in Fig. 3) with the quantum number K_a being odd. One can see that the isomers $B_b[B_b]$ and $B_c[B_c]$ cannot be distinguished, due to degeneracy of the states $\Phi^+_{J,K_a,m}$ and $\Phi^-_{J,K_a,m}$ with the same J and K_a. The energies of the A[A] and $B_a[B_a]$ species are also degenerate for $K_a \neq 0$. However, the states for $K_a = 0$ belong to the A[A] species if J is even, and to the $B_a[B_a]$ species, if J is odd. Thus, these two species can be distinguished from each other by their energies corresponding to $K_a = 0$.

The rotational spectra of different nuclear spin isomers for the analogues C_2X_4 are shown in Fig. 4.

Each rotational state J_{K_a,K_c} of ethylene (left), fully deuterated ethylene (middle) and tetrafluoro ethylene (right) can be assigned to a distinct nuclear spin isomer. Furthermore, one can see that, although the degeneracy in K_a is removed, the four nuclear spin isomers can still be grouped into two classes being similar in energy: The A[A] and $B_a[B_a]$ isomers occur in pairs of even K_a; the exception is $K_a = 0$, where these isomers are alternating with J. The $B_b[B_b]$ and $B_c[B_c]$ species appear in pairs of odd K_a.

For partially deuterated ethylene, i.e., [1,1-$^2H_2$]ethylene and (*Z*)-[1,2-$^2H_2$]ethylene (see Fig. 1(e) and 1(f)), the situation is no less interesting. Although the spectra of the two isotopomers are almost the same, they have different nuclear spin isomers, as shown in Fig. 5.

For [1,1-$^2H_2$]ethylene (left side of Fig. 5), all rotational states with even K_a, regardless of J, belong to one isomer and all states with odd K_a to the other. The nuclear spin isomers of (*Z*)-[1,2-$^2H_2$]ethylene (right side of Fig. 5), on the other hand can be distinguished by even and odd values of J for $K_a = 0$; for $K_a \neq 0$ both isomers have rotational states with even and odd J and K_a. The energy eigenvalues of these isomers are different, so we expect that they show very different alignment dynamics. This may open a possibility to distinguish isotopomers via their nuclear spin.

III. THEORY OF NON-ADIABATIC ALIGNMENT OF ASYMMETRIC TOP MOLECULES

To investigate the effect of the nuclear spin on the rotational dynamics, we simulate the field-free alignment for every distinct nuclear spin isomer after interacting with a moderately strong, non-resonant laser pulse. If a molecule is exposed to a short (compared to the time-scale of rotational motions) laser pulse with a frequency chosen to be non-resonant to any molecular transition, the molecule interacts with the laser pulse approximately via its dynamic polarizability. Under such conditions, the laser pulse excites only rotational states; the system remains in its electronic and vibrational ground state. Typical pulse parameters in alignment experiments are $I = 10\,\mathrm{TW/cm^2}$ for pulse intensities, $\sigma = 100\,\mathrm{fs}$ for pulse lengths and $\lambda = 800\,\mathrm{nm}$ for the wave length of the laser light.[14] The Hamiltonian for this kind of interaction reads[18,19,42]

$$\hat{H}^{\mathrm{int}} = -\frac{1}{4}\boldsymbol{\epsilon}^{\dagger}(t)\cdot\boldsymbol{\alpha}\cdot\boldsymbol{\epsilon}(t)\,, \tag{3.1}$$

with $\boldsymbol{\epsilon}$ denoting the polarization and the shape of the envelope of the laser pulse and $\boldsymbol{\alpha}$ the dynamic polarizability tensor.

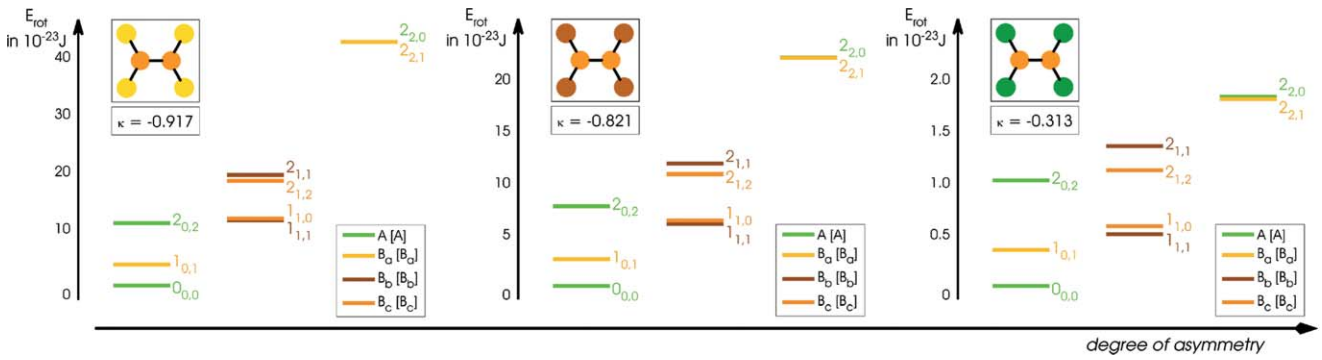

FIG. 4. Rotational spectra of ethylene (left), fully deuterated ethylene (middle) and tetrafluoro ethylene (right) for $J = 0, 1, 2$. The rotational states are labeled by J_{K_a,K_c}. Different colors correspond to different nuclear spin isomers being defined by different combinations of rotational symmetries $\boldsymbol{\Gamma}^{\mathrm{rot}}$ and nuclear spin symmetries $\boldsymbol{\Gamma}^{\mathrm{nu.sp}}$. The nomenclature of the legend is $\boldsymbol{\Gamma}^{\mathrm{rot}}[\boldsymbol{\Gamma}^{\mathrm{nu.sp}}]$.

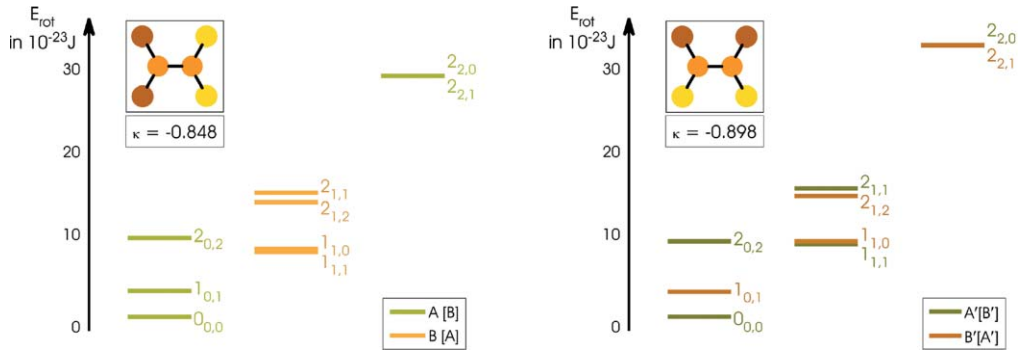

FIG. 5. Rotational spectra of [1,1-^{2}H$_2$]ethylene (left) and (*Z*)-[1,2-^{2}H$_2$]ethylene (right) for $J = 0, 1, 2$. The rotational states are labeled by J_{K_a,K_c}. Different colors correspond to different nuclear spin isomers being defined by different combinations of rotational symmetries $\mathbf{\Gamma}^{\text{rot}}$ and nuclear spin symmetries $\mathbf{\Gamma}^{\text{nu.sp}}$. The nomenclature of the legend is $\mathbf{\Gamma}^{\text{rot}}[\mathbf{\Gamma}^{\text{nu.sp}}]$.

Although its components depend on the frequency of the laser field, it converges to the static polarizability, if the frequency of the laser pulse is sufficiently low. In case of a field polarized in $\boldsymbol{e}_Z$-direction, where $\boldsymbol{\epsilon} = \epsilon(t) \cdot \boldsymbol{e}_Z$ this Hamiltonian reduces (up to a constant) to

$$\hat{H}^{\text{int}} = -|\epsilon(t)|^2 \left(\alpha^{2,0}\mathcal{D}^2_{0,0} + \alpha^{2,2}\left(\mathcal{D}^2_{0,2} + \mathcal{D}^2_{0,-2}\right)\right). \quad (3.2)$$

Here, the irreducible components of the polarizability $\alpha^{2,k}$ are defined by

$$\alpha^{2,0} = \frac{2\alpha_{aa} - \alpha_{bb} - \alpha_{cc}}{12} \quad (3.3a)$$

and

$$\alpha^{2,2} = \frac{\alpha_{bb} - \alpha_{cc}}{4\sqrt{6}}, \quad (3.3b)$$

where α_{ii}, $i = a, b, c$ refer to the principal axes system from Fig. 2; the symbols $\mathcal{D}^J_{m,k}$ denote the Wigner rotation matrices as a function of the Euler angles.[43] The values of the irreducible components of the dipole polarizability for the molecules considered here are tabulated in Table III. For ethylene, its isotopologues and tetrafluoro ethylene, they have been obtained from Refs. 36, 37, and 44; for allene, quantum chemical calculations have been performed using the program package GAUSSIAN 03 (Ref. 38) on CCSD(T) level of theory with an augmented correlation-consistent triple zeta basis.

In order to quantify the effect of the non-resonant laser pulse on the molecular system, we solve the time-dependent Schrödinger equation

$$\mathrm{i}\hbar\frac{\partial}{\partial t}\Psi(t) = \left(\hat{H}^{\text{rot}} + \hat{H}^{\text{int}}\right)\Psi(t) \quad (3.4)$$

following the strategy of Gershnabel and Averbukh.[31] We make use of the impulse approximation, i.e., we set $\hat{H}^{\text{rot}} = 0$ during the interaction. This allows us to write the time-dependent wave function in Eq. (3.4) as

$$\Psi(t_{0+}) = \exp\left(-\frac{\mathrm{i}}{\hbar}\int_{t_{0-}}^{t_{0+}} \hat{H}^{\text{int}}\mathrm{d}t\right)\Psi(t_{0-}), \quad (3.5)$$

where $\Psi(t_{0-})$ denotes the wave function before and $\Psi(t_{0+})$ the wave function at the end of the laser pulse. Note, that $\Psi(t_{0+})$ is no longer a rotational eigenstate but a wave packet consisting of the rotational states which have been excited by the short laser pulse. We expand $\Psi(t_{0+})$ into eigenfunctions $\Phi^{\mathbf{\Gamma}}_{J,\tau,m}$ of the free asymmetric rotor and calculate the expansion coefficients numerically. Therefore, we introduce an artificial parameter ξ having at time t_{0^-} the value $\xi = 0$ and at time t_{0^+} the value $\xi = 1$, and define

$$\Psi_\xi = \exp\left(-\mathrm{i}\left(\beta^{2,0}\mathcal{D}^2_{0,0} + \beta^{2,2}(\mathcal{D}^2_{0,2} + \mathcal{D}^2_{0,-2})\,\xi\right)\right)\Psi(t_{0-}), \quad (3.6)$$

with

$$\beta^{2,k} = \frac{\alpha^{2,k}}{\hbar}\int_{t_{0-}}^{t_{0+}} |\epsilon(t)|^2\mathrm{d}t \quad k = 0, 2\,. \quad (3.7)$$

We choose a Gauss-shaped laser pulse

$$\epsilon(t) = \epsilon_0 \exp\left(-2\ln 2\frac{t^2}{\sigma^2}\right), \quad (3.8)$$

with a FWHM of $\sigma = 100$ fs and different maximal intensities $I_{\text{max}} = 1/2c\varepsilon_0|\epsilon_0|^2$, as discussed below.

We expand the function Ψ_ξ into the free rotor eigenstates $\Phi^{\mathbf{\Gamma}}_{J,\tau,m_0}$, that is, we write

$$\Psi_\xi = \sum_{J,\tau\in\mathbf{\Gamma}} c^{\mathbf{\Gamma}}_{J,\tau,m_0}(\xi)\Phi^{\mathbf{\Gamma}}_{J,\tau,m_0}, \quad (3.9)$$

for all rotational symmetries $\mathbf{\Gamma}$ separately. Note, that in case of a linear polarized laser field $m = m_0$ is a conserved quantity. Utilizing this ansatz in Eq. (3.6) and differentiating with respect to ξ leads to a system of coupled equations for the coefficients $c^{\mathbf{\Gamma}}_{J,\tau,m_0}$, given explicitly by

$$\begin{aligned}\frac{\mathrm{d}c^{\mathbf{\Gamma}}_{J',\tau',m_0}(\xi)}{\mathrm{d}\xi} = \frac{1}{\mathrm{i}}\sum_{J,\tau\in\mathbf{\Gamma}} c^{\mathbf{\Gamma}}_{J,\tau,m_0}(\xi)\big(&\beta^{2,0}\langle J',\tau',m_0|\mathcal{D}^2_{0,0}|J,\tau,m_0\rangle \\ &-\beta^{2,2}\langle J',\tau',m_0|\mathcal{D}^2_{0,2}|J,\tau,m_0\rangle \\ &-\beta^{2,2}\langle J',\tau',m_0|\mathcal{D}^2_{0,-2}|J,\tau,m_0\rangle\big)\end{aligned} \quad (3.10)$$

or in matrix form

$$\frac{\mathrm{d}\boldsymbol{c}_{\mathbf{\Gamma}}(\xi)}{\mathrm{d}\xi} = \frac{1}{\mathrm{i}}\boldsymbol{H}^{\text{int}}_{\mathbf{\Gamma}}\cdot\boldsymbol{c}_{\mathbf{\Gamma}}(\xi)\,. \quad (3.11)$$

Although the matrix $\boldsymbol{H}^{\text{int}}_{\mathbf{\Gamma}}$ contains non-vanishing elements between states of different J and τ, the field cannot induce transitions between different nuclear spin isomers and thus

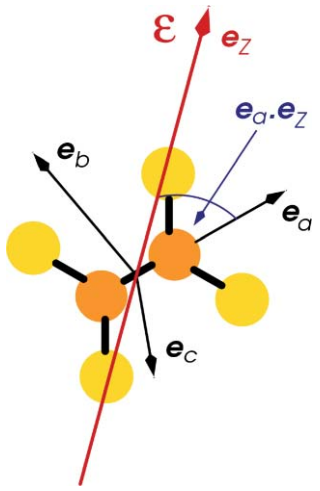

FIG. 6. Sketch of the direction cosines defined in Eq. (3.15).

Eq. (3.10) can be solved for each rotational symmetry $\mathbf{\Gamma}$ separately. This is understood taking into account group theoretical arguments; a detailed discussion is given in Appendix B. Since the asymmetric top eigenfunctions are a superposition of symmetric top eigenstates, the matrix $\boldsymbol{H}^{\mathrm{int}}_{\mathbf{\Gamma}}$ contains the elements

$$\begin{aligned}&\langle J', K', m_0|\mathcal{D}^2_{0\nu}|J, K, m_0\rangle\\ &\quad=(-1)^{K+m_0}\sqrt{2J+1}\sqrt{2J'+1}\\ &\qquad\times\begin{pmatrix} J' & 2 & J\\ -m_0 & 0 & m_0\end{pmatrix}\begin{pmatrix} J' & 2 & J\\ -K' & \nu & K\end{pmatrix}\end{aligned}\tag{3.12}$$

with $\nu = 0, \pm 2$. The $3j$-symbols in Eq. (3.12) are only nonzero, if

$$|J-2|\leq J'\leq J+2\quad\text{and}\quad K'=K, |K\pm 2|\,.\tag{3.13}$$

After the interaction with the laser pulse, the molecules evolve freely and the time-dependent wave function $\Psi^{\mathbf{\Gamma}}(t)$ can be expressed as follows

$$\Psi^{\mathbf{\Gamma}}(t)=\sum_{J,\tau\in\mathbf{\Gamma}} c^{\mathbf{\Gamma}}_{J,\tau,m_0}\exp\left(-\frac{\mathrm{i}}{\hbar}E^{\mathbf{\Gamma}}_{J,\tau}t\right)\Phi^{\mathbf{\Gamma}}_{J,\tau,m_0},\tag{3.14}$$

where we have set $t_{0^+}=0$. The coefficients $c^{\mathbf{\Gamma}}_{J,\tau,m_0}\equiv c^{\mathbf{\Gamma}}_{J,\tau,m_0}(\xi=1)$ are found from the solution of Eq. (3.10). To analyze the wave packet Eq. (3.14) and the degree of the post pulse alignment, we calculate the expectation value

$$\langle|\boldsymbol{e}_a\cdot\boldsymbol{e}_Z|^2\rangle=\frac{1}{3}+\frac{2}{3}\langle\mathcal{D}^2_{0,0}\rangle\,,\tag{3.15}$$

i.e., the degree of alignment of the principal axis $\boldsymbol{e}_a$ with respect to the polarization $\boldsymbol{e}_Z$ of the laser pulse, as illustrated in Fig. 6.

Finally, we calculate the (classical) thermal average, i.e.,

$$\langle\langle|\boldsymbol{e}_a\cdot\boldsymbol{e}_Z|^2\rangle\rangle_{\mathbf{\Gamma}}=\sum_{J_0,\tau_0\in\mathbf{\Gamma},m_0}\frac{\exp(-E_{J_0,\tau_0}/k_BT)}{Z^{\mathrm{rot}}_{\mathbf{\Gamma}}}\langle|\boldsymbol{e}_a\cdot\boldsymbol{e}_Z|^2\rangle_{J_0,\tau_0,m_0}.\tag{3.16}$$

The triple J_0, τ_0, m_0 characterizes the initial rotational state $\Phi^{\mathbf{\Gamma}}_{J_0,\tau_0,m_0}$ of the representative in the thermal system; $Z^{\mathrm{rot}}_{\mathbf{\Gamma}}$ denotes the Maxwell-Boltzmann partition function for a given rotational symmetry.

In the following, we will present the results for the alignment factor Eq. (3.16) for the different nuclear spin isomers of the molecules considered in this study. In order to compare the rotational dynamics of the different molecules, we introduce scaled variables with

$$E'=\frac{\mathfrak{B}+\mathfrak{C}}{2},\tag{3.17a}$$

$$T'=\frac{E'}{k_{\mathrm{B}}},\tag{3.17b}$$

$$t'=\frac{2\pi\hbar}{\mathfrak{B}+\mathfrak{C}},\tag{3.17c}$$

for energy, temperature and time, respectively.

IV. NUCLEAR SPIN SELECTIVE ALIGNMENT

A. Alignment of the four nuclear spin isomers of ethylene

The alignment of asymmetric top molecules like ethylene has been measured.[14] The post pulse alignment signal can be understood as a mixture of the alignment factors of the nuclear spin isomers according to their statistical weight. The left hand side of Fig. 7 shows alignment of ethylene under such conditions.

It displays the expectation value $\langle\langle|\boldsymbol{e}_a\cdot\boldsymbol{e}_Z|^2\rangle\rangle$ as a function of time and reproduces the results of Rouzee *et al.*[14] However, from the statistical averaged alignment factor, one can not obtain any information how the four nuclear spin isomers of ethylene, which we have identified in Sec. II, behave individually.

That they do behave very differently is shown in the right panel of Fig. 7, where the individual alignment factors of the four nuclear spin isomers are shown. The alignment immediately after the interaction ($t\approx 1/10t'$) is almost the same for all nuclear spin isomers. For later times, they show different behavior: we see that at $t\approx 1/4t'$ the species $\mathrm{B_a[B_a]}$ (yellow line) are aligned with respect to the $\boldsymbol{e}_Z$-axis while the A[A] species (green line) shows anti-alignment. At $t\approx 3/4t'$ this situation is reversed. For the $\mathrm{B_b[B_b]}$ (brown line) and $\mathrm{B_c[B_c]}$ (orange line) species, we observe a similar but less distinct behavior: slightly before $t\approx 1/4t'$ the species $\mathrm{B_c[B_c]}$ shows alignment, while the $\mathrm{B_b[B_b]}$ species shows anti-alignment; slightly after $t\approx 1/4t'$ the opposite occurs. As for the A[A] and $\mathrm{B_a[B_a]}$ species, this behavior is repeated in reverse order at $t\approx 3/4t'$. We also note, that the alignment of the isomers A[A] and $\mathrm{B_a[B_a]}$ can become considerably larger than the maximal alignment of the statistical mixture of all nuclear spin isomers.

In the following, we analyze the alignment of individual nuclear spin isomers of ethylene and its analogues by comparing it with the alignment of the symmetric top allene, and discuss possible applications of the nuclear spin selective alignment.

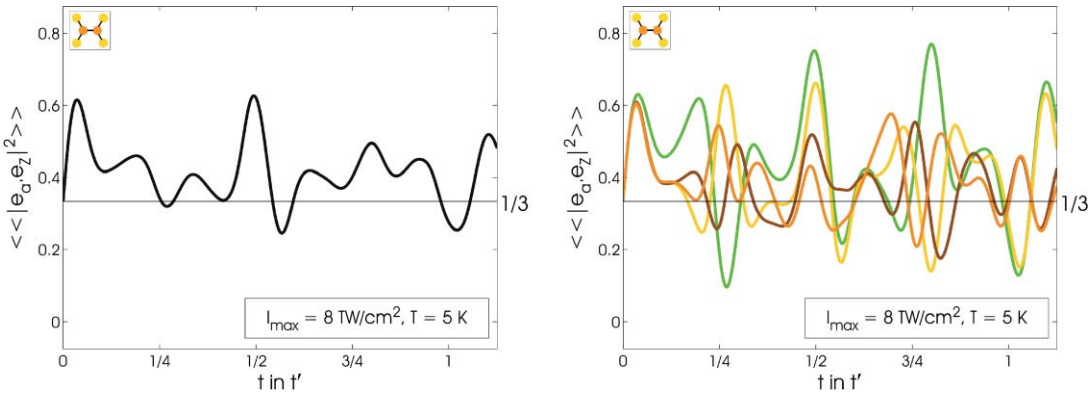

FIG. 7. Left panel: Statistical averaged alignment factor $\langle\langle|\boldsymbol{e}_a \cdot \boldsymbol{e}_Z|^2\rangle\rangle$ of ethylene for $T = 5\,\mathrm{K}$, a maximal pulse intensity of $I_{\max} = 8\,\mathrm{TW/cm^2}$ and a pulse width $\sigma = 100\,\mathrm{fs}$. Right panel: alignment factors for the four nuclear spin isomers of ethylene for the same conditions. The time is given in units of $t' = 18.24\,\mathrm{ps}$. Here, the green curve represents isomer A[A], the yellow curve represents isomer B_a[B_a], and the brown and orange curves show the isomers B_b[B_b] and B_c[B_c], respectively.

B. Symmetric vs. asymmetric tops: Allene and ethylene

As shown in Sec. II, the symmetric top molecule allene has the same nuclear spin isomers as ethylene. By comparing the rotational dynamics of allene and ethylene, we can directly study the effect of asymmetry on the alignment signal for each isomer. The alignment factor $\langle\langle|\boldsymbol{e}_a \cdot \boldsymbol{e}_Z|^2\rangle\rangle$ for the nuclear spin isomers of allene for $I_{\max} = 7.2\,\mathrm{TW/cm^2}$ and $T = 1.6\,\mathrm{K}$ (in scaled units: $\beta^{20} = 6.8$ and $T/T' = 3.8$) is shown in Fig. 8.

Since allene is a symmetric top, the alignment factor has exact revivals with the revival time $t_{\mathrm{rev}} = t' = \hbar\pi/\mathfrak{B} = 56.69\,\mathrm{ps}$.

For a symmetric top molecule, $\alpha^{2,2} = 0$ and the interaction with the laser pulse Eq. (3.2) reduces to

$$\hat{H}^{\mathrm{int}} = -|\epsilon(t)|^2 \alpha^{2,0} \mathcal{D}^2_{0,0}\,. \tag{4.1}$$

As a consequence, the quantum number $K = K_0$ is preserved during the interaction. The wave function after the interaction can thus be written as

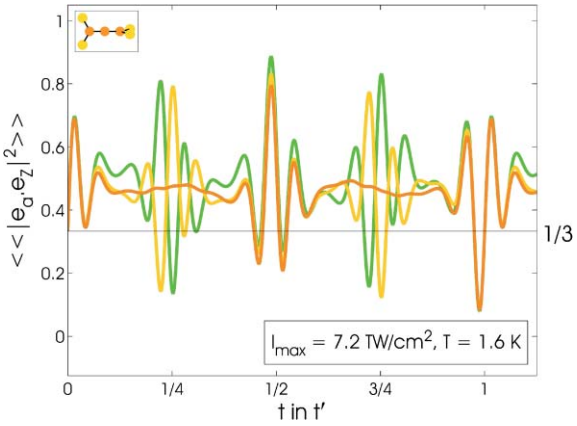

FIG. 8. The alignment factor $\langle\langle|\boldsymbol{e}_a \cdot \boldsymbol{e}_Z|^2\rangle\rangle$ for the nuclear spin isomers of allene given in units of $t' = 56.69\,\mathrm{ps}$. As before, the nuclear spin isomers A[A] and B_a[B_a] are represented with green and yellow curves, respectively. The isomers B_b[B_b] and B_c[B_c] have identical alignment factors depicted in orange.

$$\Psi^{\Gamma}(t) = \sum_J c^{\Gamma}_{J,0,m_0} \exp\left(-\frac{\mathrm{i}}{\hbar} E_{J,0} t\right) \Phi_{J,0,m_0}, \tag{4.2}$$

for $K_0 = 0$. For rotational states with even J_0, only even J contribute to $c^{\Gamma}_{J,0,m_0}$; if J_0 is odd, only odd J are contained in $c^{\Gamma}_{J,0,m_0}$. For $K_0 \neq 0$,

$$\Psi^{\Gamma} = \sum_J c^{\Gamma}_{J,K_0,m_0} \exp\left(-\frac{\mathrm{i}}{\hbar} E_{J,K_0} t\right) \Phi^{\pm}_{J,K_0,m_0}\,. \tag{4.3}$$

Since $\langle J, -K_0, m_0|\mathcal{D}^2_{0,0}|J, K_0, m_0\rangle = 0$, the alignment factor for the symmetric top states Φ^{+}_{J,K_0,m_0} and Φ^{-}_{J,K_0,m_0} is identical. The nuclear spin isomers B_b[B_b] and B_c[B_c] can therefore, not be distinguished by their alignment factor. However, rotational states with $K_0 = 0$ belong to the A[A] isomer (green line), if J is even and to isomer B_a[B_a] (yellow line) if J is odd. Since rotational wave packets with even and odd J have different alignment factors, these two isomers can be distinguished from each other and from isomers B_b[B_b] and B_c[B_c] (orange line). One can write for $K_0 = 0$,

$$\langle|\boldsymbol{e}_a \cdot \boldsymbol{e}_Z|^2\rangle(t) = \langle|\boldsymbol{e}_a \cdot \boldsymbol{e}_Z|^2\rangle_0 + \langle|\boldsymbol{e}_a \cdot \boldsymbol{e}_Z|^2\rangle_c(t), \tag{4.4}$$

where the first term,

$$\langle|\boldsymbol{e}_a \cdot \boldsymbol{e}_Z|^2\rangle_0 = \frac{1}{3} + \frac{2}{3}\sum_J |c^{\Gamma}_{J,0,m_0}|^2 \cdot (-1)^{m_0}(2J+1) \times \begin{pmatrix} J & 2 & J \\ -m_0 & 0 & m_0 \end{pmatrix}\begin{pmatrix} J & 2 & J \\ 0 & 0 & 0 \end{pmatrix}, \tag{4.5}$$

is the degree of time-independent alignment. The coherence term[45] $\langle|\boldsymbol{e}_a \cdot \boldsymbol{e}_Z|^2\rangle_c$ describes the time-dependent part of the alignment factor, given by

$$\langle|\boldsymbol{e}_a \cdot \boldsymbol{e}_Z|^2\rangle_c(t) = \frac{4}{3}\,\mathfrak{Re}\left\{\sum_J \left(c^{\Gamma}_{J+2,0,m_0}\right)^* c^{\Gamma}_{J,0,m_0} \cdot (-1)^{m_0} \times \sqrt{(2J+1)(2J+3)}\begin{pmatrix} J+2 & 2 & J \\ -m_0 & 0 & m_0 \end{pmatrix} \begin{pmatrix} J+2 & 2 & J \\ -K' & \nu & K \end{pmatrix} \exp\left(-\mathrm{i}\frac{\mathfrak{B}}{\hbar} 2(2J-3)t\right)\right\}. \tag{4.6}$$

It can be seen from Eq. (4.6) that $\langle|\boldsymbol{e}_a \cdot \boldsymbol{e}_Z|^2\rangle_c$ is repeated exactly after the revival period $t_{\rm rev} = t' = \hbar/\mathfrak{B}\pi$. Moreover, after half of the revival time,

$$\langle|\boldsymbol{e}_a \cdot \boldsymbol{e}_Z|^2\rangle_c \left(t + \frac{t_{\rm rev}}{2}\right) = -\langle|\boldsymbol{e}_a \cdot \boldsymbol{e}_Z|^2\rangle_c(t). \tag{4.7}$$

At $t \approx 1/4t'$ and $t \approx 3/4t'$, the factor $\exp(i\pi J)$ in Eq. (4.6) assures that states with even and odd J have opposite sign, i.e., states with even J (A[A] isomer) show alignment while states with odd J are anti-aligned and vice-versa. The A[A] and B_a[B_a] isomer of allene behave very similar to the two nuclear spin isomers of homo-nuclear diatomic molecules, for which nuclear spin selective alignment has been observed and investigated in detail.[28]

Also for $K_0 \neq 0$, states with even and odd J show differences in the alignment signal at $t \approx 1/4t'$. Here, however, each nuclear spin isomer has rotational states with even and odd J. Alignment and anti-alignment thus cancel each other and the resulting alignment is approximately $\langle|\boldsymbol{e}_a \cdot \boldsymbol{e}_Z|^2\rangle_0$.

The alignment factors of the nuclear spin isomers of ethylene (Fig. 7) shows that at $t \approx 1/4t'$ and $t \approx 3/4t'$ the isomers A[A] and B_a[B_a] are also aligned and anti-aligned, respectively, as for a symmetric top rotor. However, due to its asymmetry, exact revivals of the rotational wave packets do not occur for ethylene. Moreover K is not preserved for an asymmetric top and thus the rotational wave packets contain states with different K. As a consequence, the alignment factors of the isomers B_b[B_b] and B_c[B_c] also differ.

A quantitative comparison between ethylene and allene is shown in Fig. 9. Here, we show the difference of the alignment factors

$$D_{aZ}(\boldsymbol{\Gamma}_1, \boldsymbol{\Gamma}_2) = \mathrm{abs}\left(\langle\langle|\boldsymbol{e}_a \cdot \boldsymbol{e}_Z|^2\rangle\rangle_{\boldsymbol{\Gamma}_1} - \langle\langle|\boldsymbol{e}_a \cdot \boldsymbol{e}_Z|^2\rangle\rangle_{\boldsymbol{\Gamma}_2}\right), \tag{4.8}$$

with $\boldsymbol{\Gamma}_i$ denoting the rotational symmetry, for the two pairs ($\boldsymbol{\Gamma}_1 = \mathrm{A}, \boldsymbol{\Gamma}_2 = \mathrm{B_a}$) (green and yellow lines in Fig. 7 and 8) and ($\boldsymbol{\Gamma}_1 = \mathrm{B_b}, \boldsymbol{\Gamma}_2 = \mathrm{B_c}$) (brown and orange lines in Fig. 7, orange line in Fig. 8). The function $D_{aZ}(\mathrm{A}, \mathrm{B_a})$ for allene, which is depicted in blue lines in Fig. 9 upper panel, is periodic in t'; it is maximal close to each quarter revival; at half and full revivals $D_{aZ}(\mathrm{A}, \mathrm{B_a})$ remains approximately zero. Also for ethylene $D_{aZ}(\mathrm{A}, \mathrm{B_a})$ becomes maximal close to quarter revivals, while it remains close to zero at approximately half and full revivals. Compared to allene, the difference $D_{aZ}(\mathrm{A}, \mathrm{B_a})$ of ethylene is less pronounced. Additionally, for larger t ($t \approx 3/4t', 5/4t', 7/4t'$), the peaks of $D_{aZ}(\mathrm{A}, \mathrm{B_a})$ decrease. The structures around quarter revivals become broader and are shifted from the quarter revivals towards slightly smaller and larger times. The reason therefore is that, for an asymmetric top, the rotational wave packet contain states with different K_a and the J-type revivals observed for a symmetric top are no longer exact revivals. Coherences between states with different K_a lead to the shifts and the broadening of the quasi-revival structures.[46] We also found that the decrease and shifts of the peaks of $D_{aZ}(\mathrm{A}, \mathrm{B_a})$ is larger for higher intensities; it arises due to the excitation of eigenstates with larger J, since those states have a larger asymmetry splitting and thus a larger mixing of symmetric top states with different K_a. As we also study molecules with higher asymmetry, where the described effect is even larger, we will limit our further investigations on times $t < t'$. The difference $D_{aZ}(\mathrm{B_b}, \mathrm{B_c})$ shown in the lower panel in Fig. 9 is zero for allene, since the B_b[B_b] and the B_c[B_c] isomers have the same alignment factors (see Fig. 8). For ethylene, $D_{aZ}(\mathrm{B_b}, \mathrm{B_c})$ is non-zero. The difference between the B_b[B_b] and B_c[B_c] isomers also becomes maximal close to quarter revivals. Due to the asymmetry of the molecule, this difference is most pronounced at $1/4t'$ and decreases for larger times.

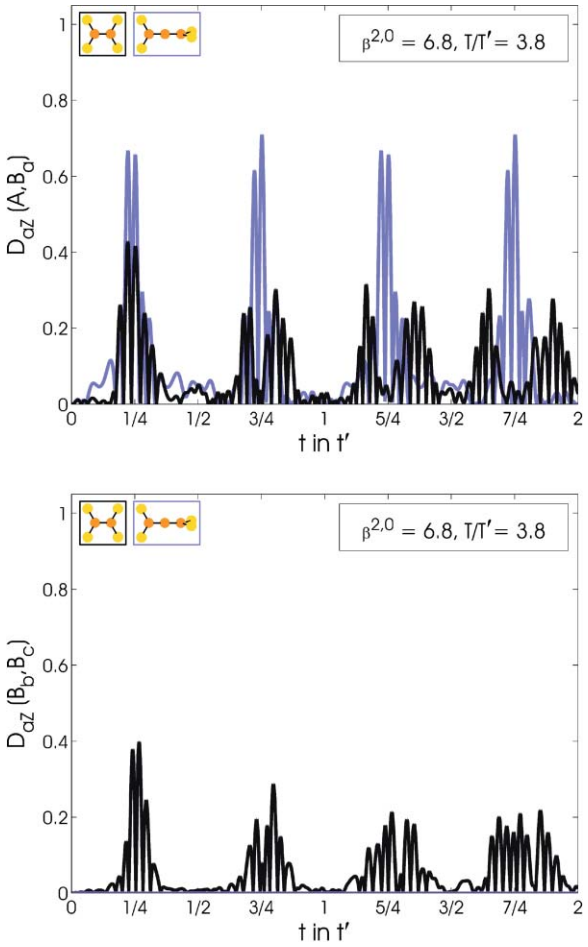

FIG. 9. Representation of $D_{aZ}(\boldsymbol{\Gamma}_1, \boldsymbol{\Gamma}_2)$ with ($\boldsymbol{\Gamma}_1 = \mathrm{A}, \boldsymbol{\Gamma}_2 = \mathrm{B_a}$) (top) and ($\boldsymbol{\Gamma}_1 = \mathrm{B_b}, \boldsymbol{\Gamma}_2 = \mathrm{B_c}$) (bottom) for ethylene (black lines) and allene (blue lines). The laser intensity and rotational temperature in scaled units are $\beta^{2,0} = 6.8$ and $T/T' = 3.8$. For ethylene this corresponds to $I_{\rm max} = 20\ \mathrm{TW/cm^2}$ and $T = 5$ K, for allene to $I_{\rm max} = 7.2\ \mathrm{TW/cm^2}$ and $T = 1.6$ K.

C. The influence of pulse intensity and asymmetry of the rotors

In the following, we investigate how the intensity of the interaction affects the alignment of nuclear spin isomers of molecules with increasing asymmetry, that is for ethylene ($\kappa = -0.917$), for fully deuterated ethylene ($\kappa = -0.821$) and for tetrafluoro ethylene ($\kappa = -0.313$). On the right hand side of Fig. 10, we show the maximal degree of alignment for each nuclear spin isomer as function of the intensity $I_{\rm max}$ of the laser pulse. To compare the alignment of the different molecules, the temperature is chosen as $T/T' = 3.8$.

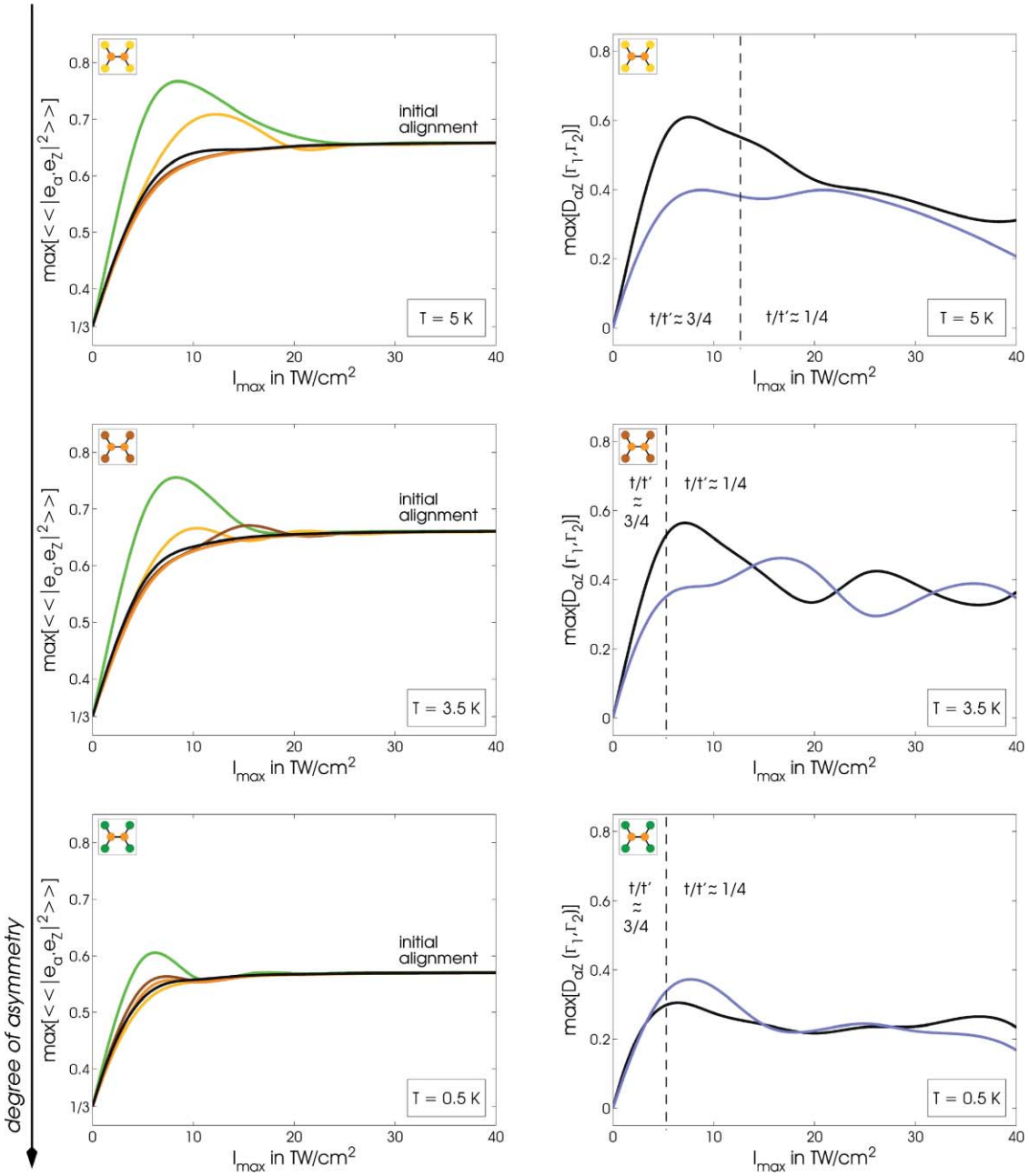

FIG. 10. Comparison of the maximal degree of alignment (left) and the maximal difference $\max[D_{aZ}(\mathbf{\Gamma}_1, \mathbf{\Gamma}_2)]$ (right) as a function of the maximal laser intensity $I_{\max}$ between the A[A]/B_a[B_a] species (black) and the B_b[B_b]/B_c[B_c] species (light blue). In the left figures, the colors correspond to the same nuclear spin isomers as in Fig. 7; the black line corresponds to the statistical average. Note, that interaction strengths for all molecules are similar, i.e., the effect of the maximal intensity can be directly compared. The temperatures are chosen such that $T/T' = 3.8$ for all molecules.

For the statistical mixture of all nuclear spin isomers of ethylene (black line in top left panel of Fig. 10), the degree of alignment increases monotonically with increasing intensity and converges to the value 0.66. The maximal alignment is the initial alignment, which occurs shortly after the interaction (see $t \approx 1/10t'$ in Fig. (7)) The individual nuclear spin isomers, in particular the isomers A[A] (green lines) and B_a[B_a] (yellow lines) show a different behavior: their maximal alignment is considerably larger (0.76 for the A[A] isomer) than that of the statistical mixture. Moreover, maximal alignment is obtained at moderate intensities, i.e., at $I_{\max} \approx 8\,\mathrm{TW/cm^2}$ for the A[A] isomer and $I_{\max} \approx 10\,\mathrm{TW/cm^2}$ for the B_a[B_a] isomer. It is interesting to note, that the maximal alignment for these intensities does not occur immediately after the interaction, but at $t \approx 1/2t'$, as it can also be seen in the right panel of Fig. 7. For large intensities, the maximal alignment of the isomers A[A] and B_a[B_a] converges to the maximal alignment of the statistical mixture and occurs directly after the interaction. A similar effect has been reported for the alignment factor of linear molecules,[47] where the maximal alignment, also depends on the interaction strength in a non-monotonic way. Also for linear molecules the alignment factor is maximal at a half revival time (at least for moderate temperatures). We have seen in Sec. IV B that the rotational dynamics of the A[A] and B_a[B_a] isomers of a prolate symmetric or asymmetric top is similar to the dynamics of the nuclear spin isomers

of a linear molecule[28] - here, again we observe that these isomers behave similar to a linear molecule while the intensity dependence of the alignment factor for the isomers $B_b[B_b]$ and $B_c[B_c]$ (brown and orange lines in Fig. 10) is similar to that of the statistical mixture.

By comparing the maximal alignment of ethylene with fully deuterated ethylene (middle panel of Fig. 10) and with tetrafluoro ethylene (bottom of Fig. 10), we observe that the maximal alignment of the statistical mixture (black lines) is slightly reduced: from 0.66 for ethylene to 0.57 for tetrafluoro ethylene. For the A[A] isomer, we see a non-monotonic behavior for all three molecules, but the maximal alignment at moderate intensities ($I_{\max} \approx 8\,\mathrm{TW/cm^2}$) is considerably reduced with increasing asymmetry of the molecule. With increasing asymmetry, also the A[A] isomer does not resemble the corresponding isomer of a linear molecule.

On the right hand side of Fig. 10, we show the maximal difference between the alignment factors, i.e.,

$$\max\left[D_{aZ}(\mathbf{\Gamma}_1, \mathbf{\Gamma}_2)\right], \tag{4.9}$$

for the pairs ($\mathbf{\Gamma}_1 = \mathrm{A}, \mathbf{\Gamma}_2 = \mathrm{B_a}$) depicted in black lines, and ($\mathbf{\Gamma}_1 = \mathrm{B_b}, \mathbf{\Gamma}_2 = \mathrm{B_c}$) depicted in blues lines, as a function of the pulse intensity $I_{\max}$. It turns out, that for ethylene (top) the largest difference is obtained for moderate intense laser pulses, i.e., $I_{\max} \approx 8\,\mathrm{TW/cm^2}$. The difference in the alignment factors for the pair (A, B_a) is always larger than for the pair (B_b, B_c). The points in time where the maximal differences occur are shifted for higher intensities from $t \approx 3/4t'$ to $t \approx 1/4t'$; again for the reason of exciting higher J-states at higher intensities, which gives rise to different types of coherences and to the reduction of J-type revivals.

The results for $\max[D_{aZ}]$ for fully deuterated ethylene and tetrafluoro ethylene are slightly different than for ethylene: although the largest differences are again obtained for moderate intense laser fields ($I_{\max} \approx 8 - 9\,\mathrm{TW/cm^2}$), the point in time, where these differences occur, is shifted to $t \approx 1/4t'$ at smaller intensities. For tetrafluoro ethylene, the maximal difference is now larger for (B_b, B_c). Interestingly, the maximal value of $\max[D_{aZ}]$ for these species is relatively constant for all three molecules, and only the maximal values for (A, B_a) are reduced. Nevertheless, the differences between the alignment factors for the different nuclear spin isomers are reduced with increasing asymmetry, making it more difficult to separate these isomers for strongly asymmetric molecules.

D. Using nuclear spin selectivity to distinguish isotopomers of molecules

So far, we investigated the nuclear spin selectivity of the alignment of molecules induced by a single, short laser pulse. It has been shown for diatomic molecules[28–30] and for water[31] that a second laser pulse with properly chosen delay time can selectively enhance the rotational energy of a single isomer. This has been suggested as a first step for the separation of nuclear spin isomers, e.g., by using additional spatially inhomogeneous static or time-dependent fields.[31] The difference in the alignment of the nuclear spin isomers of ethylene and its analogues which we found here, suggests that this scheme can also applied to polyatomic molecules with more than two nuclear spin isomers. Moreover, this selectivity could also be used to distinguish isotopomers of molecules, i.e., molecules with isotopic nuclei having the same constitution, but different configurations.

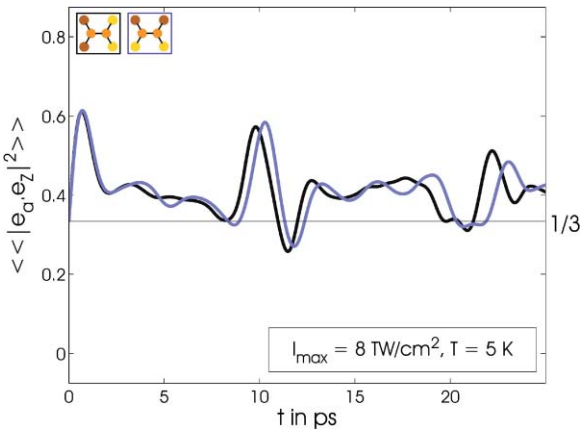

FIG. 11. The alignment factor for the statistical mixtures of [1,1-$^2H_2$]ethylene (black line) and *(Z)*-[1,2-$^2H_2$]ethylene (blue line) for $T = 5\,\mathrm{K}$ and a laser intensity of $I_{\max} = 8\,\mathrm{TW/cm^2}$.

The isotopomers [1,1-$^2H_2$]ethylene (analogue (e) in Fig. 1) and *(Z)*-[1,2-$^2H_2$]ethylene (analogue (f) in Fig. 1) provide two examples for such investigations. Their statistically averaged alignment factor for $I_{\max} = 8\,\mathrm{TW/cm^2}$ and $T = 5\,\mathrm{K}$ is shown in Fig. 11. One can see, that both isotopomers can be hardly distinguished by these statistical averaged values. However, if we take a look at the alignment factors for the individual nuclear spin isomers of these molecules, which are shown in Fig. 12 for the same set of parameters, an interesting difference between these isomers occurs at $t \approx 5\mathrm{ps}$, where the statistical averaged alignment factor in Fig. 11 implies that the distribution of the molecules is almost isotropic for both isotopomers, Fig. 12 shows that the two nuclear spin isomers of *(Z)*-[1,2-$^2H_2$]ethylene (right panel) have distinct alignment and anti-alignment, whereas the two nuclear spin isomers of [1,1-$^2H_2$]ethylene (left panel) are indeed almost isotropically distributed. A similar, but reversed situation occurs at $t \approx 20\,\mathrm{ps}$ where both nuclear spin isomers of *(Z)*-[1,2-$^2H_2$]ethylene (right panel) are isotropically distributed, while the isomers of [1,1-$^2H_2$]ethylene show alignment and anti-alignment, respectively.

Using a second laser pulse, alignment for one nuclear spin isomer of the 1,2 substituted species could be enhanced. Afterwards, one could use a spatially inhomogeneous static or an additional time-dependent field in order to separate the nuclear spin isomers of this compound and separating additionally the isotopomers from each other.[31] Thus, for isotopomers containing nuclei with non-zero spin, the nuclear spin selective alignment provides a opportunity to separate not only nuclear spin isomers but isotopomers as well.

V. SUMMARY, CONCLUSIONS, AND FUTURE PERSPECTIVES

As it has been demonstrated for diatomic molecules[28,30,48] and for water,[31] the non-adiabatic alignment

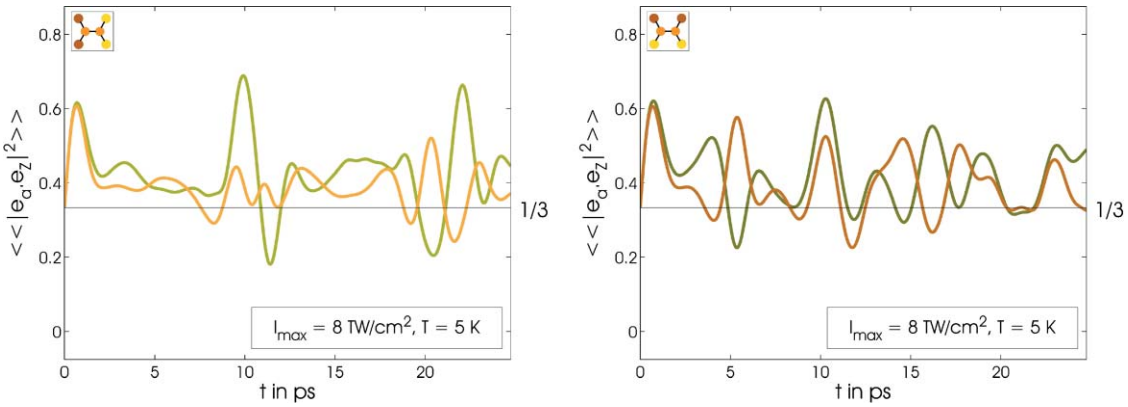

FIG. 12. The alignment factors for the nuclear spin isomers of [1,1-$^2H_2$]ethylene (left) and (*Z*)-[1,2-$^2H_2$]ethylene (right) for $I_{max} = 8\,TW/cm^2$ and $T = 5\,K$. The A[B] and B[A] isomers of [1,1-$^2H_2$]ethylene (left) are represented by light green and yellow curves, respectively. The dark green and light brown curves in the right panel correspond to the A[B] and B[A] isomers of (*Z*)-[1,2-$^2H_2$]ethylene.

of molecules depends significantly on their nuclear spin. Here, we have investigated the alignment of molecules with four distinct nuclear spin isomers: as examples we chose allene, which is a symmetric top molecule and ethylene with different substitutions as examples for asymmetric top rotors. We identified the nuclear spin isomers and the corresponding rotational eigenstates using the concept of feasible permutations of identical nuclei. We calculated the rotational wave functions and the alignment of the individual nuclear spin isomers after the interaction with a strong, non-resonant laser pulse. Immediately after the interaction, the rotational dynamics of all nuclear spin isomers of the molecules is almost the same, but they behave very differently at later times, in particular at quarter revival times.

However, revival times can be defined exactly only for symmetric top rotors. By comparing the alignment factors of ethylene and substituted ethylene with that of allene, we can relate the rotational dynamics of the four nuclear spin isomers of the molecules with increasing asymmetry to that of a symmetric top rotor with its exact rotational revivals. We find that for allene, the alignment factors of two of the four nuclear spin isomers are identical while the other pair of nuclear spin isomers (which contain rotational states with $K_a = 0$) shows the characteristic alignment versus anti-alignment at quarter revivals which is known for diatomic molecules. In contrast, for asymmetric rotors all four isomers show different time-dependent alignment.

Investigating the influence of the laser intensity on the alignment, we found that for the statistical mixture of nuclear spin isomers the degree of alignment increases monotonously with the intensity of the laser and converges to a high-intensity limit of 0.57 to 0.67, depending on the asymmetry. Moreover, maximal alignment always occurs shortly after the interaction with the laser pulse. However, two of the nuclear spin isomers, i.e., those which contain rotational states with even K_a, show considerably higher degree of alignment at moderate intensities. Here, the maximal degree of alignment does not occur immediately after the interaction, but half a revival time later. At high laser intensities, the degree of alignment converges to that of the statistical mixture. Additionally, we show that the degree of alignment itself and the difference between the alignment of the individual isomers decrease for more asymmetric molecules. In order to achieve better alignment for rotors with larger asymmetry, sequences of laser pulses could be applied as described in Refs. 27 and 47. These details will be important when one goes further and explores the possibility to enhance the alignment for a distinct nuclear spin isomer, using multiple laser pulses as described in Refs. 28–31 in order to separate them.

Finally, we explored the possibility to distinguish isotopomers via the alignment factor of their nuclear spin isomers. We demonstrated for two different two-fold deuterated analogues of ethylene that they have almost the same alignment factors if one considers the statistical mixtures of their nuclear spin isomers. However, the individual nuclear spin isomers show very different rotational dynamics. Selectively manipulating the rotational dynamics of the individual isomers by a sequence of laser pulses could thus be a first step for the separation of isotopomers which have the same mass and similar rotational constants and are thus very difficult to separate by conventional means.

For future investigations it will be interesting to go beyond rigid molecules and investigate the nuclear spin selectivity of the alignment of non-rigid molecules as it was done - without considering nuclear spin - in Refs. 49–51. This could lead to interesting new features of such molecules, including nuclear spin selectively driven molecular motors or nuclear spin selective chemical reactions, as earlier studies[52–55] imply.

ACKNOWLEDGMENTS

We thank Professor I. Averbukh, Professor J. Manz, and Professor Y. Prior for stimulating discussions.

APPENDIX A: COMMENTS ON THE DEFINITION OF NUCLEAR SPIN ISOMERS

In the literature on molecular spectroscopy[4,39] one finds that the effect of nuclear spin on the ro-contorsional spectra of molecules due to the symmetrization postulate is taken into account via statistical weights. Usually, these weights are

TABLE V. Character table for the MS group $D_{2d}(M)$. The abbreviations for the permutations are defined in Eqs. (2.2) and (A1).

$D_{2d}(M)$	E	(**d**)* (**e**)* $R_a^{3/2\pi}$	(**a**) R_a^{π}	(**b**) (**c**) $R_{3/4\pi}^{\pi}$	(**f**)* (**g**)* R_0^{π}
eq. rot.	R^0				
A_1	1	1	1	1	1
A_2	1	1	1	−1	−1
B_1	1	−1	1	1	−1
B_2	1	−1	1	−1	1
E	2	0	−2	0	0

found within the MS group of the molecule.[4] As long as one is not interested in a particular nuclear spin species, this approach is appropriate. However, for the assignment of a specific nuclear spin state to its corresponding rotational states, using the MS group can be inappropriate. Here, we will illustrate, why using MS groups can lead to ambiguities, discuss the conditions for their appearing and show that using the permutation subgroup of the MS groups instead of the MS group itself resolves them.

As we have pointed out in Sec. II, the MS group of allene is $D_{2d}(M)$. Its character table is shown in Table V,[4] where the missing abbreviations are

$$(\mathbf{d})^* = (1423)(56)^*, \tag{A1a}$$

$$(\mathbf{e})^* = (1324)(56)^*, \tag{A1b}$$

$$(\mathbf{f})^* = (12)^*, \tag{A1c}$$

$$(\mathbf{g})^* = (34)^*. \tag{A1d}$$

Allene is a prolate symmetric top, i.e., its rotational eigenfunctions are $\Phi_{J,K_a,m}$. They transform in $D_{2d}(M)$ according to

$$\mathbf{\Gamma}^{\text{rot}} = \begin{cases} A_1 \oplus A_2, & \text{if } K_a \text{ even and } K_a \bmod 4 = 0 \\ B_1 \oplus B_2, & \text{if } K_a \text{ even and } K_a \bmod 4 \neq 0 \\ E, & \text{if } K_a \text{ odd} \end{cases} \tag{A2}$$

for $K_a \neq 0$ and for $K_a = 0$

$$\mathbf{\Gamma}^{\text{rot}} = \begin{cases} A_1, & \text{if } J \text{ even} \\ A_2, & \text{if } J \text{ odd} \end{cases}. \tag{A3}$$

The symmetry of the 16 nuclear spin states of allene is in $D_{2d}(M)$

$$\mathbf{\Gamma}^{\text{nu.sp}} = 5A_1 \oplus A_2 \oplus 2B_1 \oplus 2B_2 \oplus 3E. \tag{A4}$$

The symmetrization postulate demands from the molecular states of allene

$$\mathbf{\Gamma}^{\text{mol}} = A_1 \quad \text{or} \quad B_1. \tag{A5}$$

However, we have now two possibilities to combine rotational states with nuclear spin states with appropriate symmetry to fulfill these conditions. We can, for example, combine a rotational state with A_1 symmetry with both, nuclear spin states with A_1 or B_1 symmetry. On the other hand, we could combine a nuclear spin state with A_1 symmetry with rotational spin states of A_1 *or* B_1 symmetry, which makes it impossible to define a nuclear spin isomer by a *unique* combination of rotational (or in general: spatial) and nuclear spin symmetry.

The reason for these ambiguities is, that the symmetrization postulate is not applicable for permutation-inversion operations and thus allows two irreducible representations $\mathbf{\Gamma}_{\pm}^{\text{mol}}$ for groups which contain at least one permutation-inversion operation. For MS groups, which, in addition, can be written as

$$G^{MS} = G_{MS}^{PS} \otimes \{E, E^*\}, \tag{A6}$$

where G_{MS}^{PS} denotes the permutation subgroup of the MS group, no inconsistencies occur: every irreducible representation can be denoted as $\mathbf{\Gamma}_{i,\pm}$, with $\mathbf{\Gamma}_i$ denoting the irreducible representations of the permutational subgroup. Furthermore, every nuclear spin state having in G_{MS}^{PS} symmetry $\mathbf{\Gamma}_i^{\text{nu.sp}}$ must, due to invariance of the nuclear spin under inversion, correlate with the representation $\mathbf{\Gamma}_{i,+}^{\text{nu.sp}}$ in the MS group. It then follows, that if

$$\mathbf{\Gamma}_i^{\text{rot}} \otimes \mathbf{\Gamma}_j^{\text{nu.sp}} \supseteq \mathbf{\Gamma}^{\text{mol}} \tag{A7}$$

in the permutation subgroup of the MS group, it holds in the MS group

$$\mathbf{\Gamma}_{i,\pm}^{\text{rot}} \otimes \mathbf{\Gamma}_{j,+}^{\text{nu.sp}} \supseteq \mathbf{\Gamma}_{\pm}^{\text{mol}}, \tag{A8}$$

with still having only one nuclear spin symmetry for disposal to fulfill this condition. Thus, to define a nuclear spin isomer, the symmetry $\mathbf{\Gamma}_j^{\text{nu.sp}}$ from the permutation subgroup must correlate non-ambiguously with *one* irreducible representation in the MS group. If, however, the MS group cannot be written as the direct product Eq. (A6), as for allene, the irreducible representation $\mathbf{\Gamma}_j^{\text{nu.sp}}$ correlates, in general, with two irreducible representations in the MS group. For example, for allene the correlations of $\mathbf{\Gamma}^{\text{nu.sp}}(D_{2d}(M)) \rightarrow \mathbf{\Gamma}^{\text{nu.sp}}(D_2(M))$, where $D_2(M)$ is the permutational subgroup of $D_{2d}(M)$, are

$$\left.\begin{matrix} A_1 \\ B_1 \end{matrix}\right\} \rightarrow A, \tag{A9a}$$

$$\left.\begin{matrix} A_2 \\ B_2 \end{matrix}\right\} \rightarrow B_a, \tag{A9b}$$

$$E \rightarrow \begin{cases} B_b \\ B_c \end{cases}. \tag{A9c}$$

Consequently, as seen in Sec. II B, by using the permutational subgroup $D_2(M)$, one avoids these ambiguities. In addition, there is a physical reason for using the permutational subgroup defining nuclear spin isomers, which we discuss below.

APPENDIX B: NUCLEAR SPIN ISOMERS IN ELECTROMAGNETIC FIELDS

Here, we discuss the symmetry properties of the complete Hamiltonian $\hat{H}^{\text{mol}} + \hat{H}^{\text{int}}$ in order to generalize the discussion of Gershnabel and Averbukh[31] that a laser, in general,

cannot induce transitions between different nuclear spin isomers.

If a molecule is brought into an electric and/or magnetic field, the symmetry group for its complete Hamiltonian is, in general, reduced.[56] The theoretical concepts for understanding nuclear spin isomers exposed to electromagnetic fields were developed in 1974 by Watson[57,58] after some remarks by Bunker.[56] Watson introduced the concepts of the electric field symmetry group and the magnetic field symmetry group. Here, we focus on the electric field symmetry group G^{EFS}, since, in general, it contains less symmetry elements than the magnetic field symmetry group. It cannot be formulated in general and depends on the type of interaction used to manipulate the molecule. We discuss the case of arbitrary polarization(s) of the electric field(s), where the spatial symmetry, represented by the group $K^{spatial}$ is completely lost due to the field. In addition, we ignore the possibility of additional symmetries arising from time-invariance since it is irrelevant for the aspects we discuss.[58]

The structure of the electric-field symmetry group depends on the type of interaction one uses to manipulate the molecule. Here, we use a laser field which interacts with the dipole polarizability of the molecule, whose components remain unchanged for both kind of operations, permutations and permutation-inversions of identical nuclei. The complete Hamiltonian is therefore invariant under the operations of the MS group and the EFS group is the direct product

$$G^{EFS} = K^{spatial} \otimes G^{MS}, \tag{B1}$$

with $K^{spatial} = C_1$. Thus, we have to use the MS group to identify the transitions the field is able to induce and find that they occur between states having the same symmetry in the MS group.

However, one has to be careful as this does not imply that in general the MS group is appropriate to find allowed transitions. In case of an electromagnetic field which interacts via the electric dipole moment $\boldsymbol{\mu}$ with the molecule the EFS is

$$G^{EFS} = K^{spatial} \otimes G^{PS}_{MS}, \tag{B2}$$

with $K^{spatial} = C_1$ and the permutational subgroup G^{PS}_{MS} introduced in Appendix A. The reason for the loss of the permutation-inversions as symmetry operations is, that the space-fixed components of the dipole moment operator μ_X, μ_Y, μ_Z change sign under each permutation-inversion operation but are invariant under the permutations of MS groups. As a consequence, all irreducible representations of the MS group $\boldsymbol{\Gamma}_i^{\pm}$, differing only by their characters under permutation-inversions, will coincide to one irreducible representation $\boldsymbol{\Gamma}_i$; degenerate representations will be, in general, reducible. Then, the electromagnetic field induces transitions between states, which are in the MS group $\boldsymbol{\Gamma}_i^{+}$- and $\boldsymbol{\Gamma}_i^{-}$-states. However, as we showed in Appendix A, the spatial energy levels belonging to these irreducible representations correspond to *one* nuclear spin isomer, and the laser field is therefore not able to induce transitions between different nuclear spin isomers.

[1] W. Heisenberg, Z. Phys. **41**, 239 (1927).
[2] F. Hund, Z. Phys. **42**, 93 (1927).
[3] K. F. Bonhoeffer and P. Harteck, Z. Phys. Chem. B **4**, 113 (1929).
[4] P. R. Bunker and P. Jensen, *Molecular symmetry and spectroscopy*, 2nd ed. (National Research Council of Canada, Ottawa, 2002).
[5] S. Guerin, A. Rouzée, and E. Hertz, Phys. Rev. A **77**, 041404(R) (2008).
[6] E. Hertz, A. Rouzée, S. Guérin, B. Lavorel, and O. Faucher, Phys. Rev. A **75** (2007).
[7] P. J. Ho, M. R. Miller, and R. Santra, J. Chem. Phys. **130**, 154310 (2009).
[8] L. Holmegaard, S. S. Viftrup, V. Kumarappan, C. Z. Bisgaard, H. Stapelfeldt, E. Hamilton, and T. Seideman, Phys. Rev. A **75**, 051403(R) (2007).
[9] F. Filsinger, J. Küpper, G. Meijer, L. Holmegaard, J. H. Nielsen, I. Nevo, J. L. Hansen, and H. Stapelfeldt, J. Chem. Phys. **131**, 064309 (2009).
[10] I. Nevo, L. Holmegaard, J. H. Nielsen, J. L. Hansen, H. Stapelfeldt, F. Filsinger, G. Meijer, and J. Küpper, Phys. Chem. Chem. Phys. **11**, 9912 (2009).
[11] S. Pabst and R. Santra, Phys. Rev. A **81**, 065401 (2010).
[12] E. Peronne, M. D. Poulsen, C. Z. Bisgaard, H. Stapelfeldt, and T. Seideman, Phys. Rev. Lett. **91**, 043003 (2003).
[13] M. D. Poulsen, E. Peronne, H. Stapelfeldt, C. Z. Bisgaard, S. S. Viftrup, E. Hamilton, and T. Seideman, J. Chem. Phys. **121**, 783 (2004).
[14] A. Rouzée, V. Boudon, B. Lavorel, and O. Faucher, Phys. Rev. A **73**, 033418 (2006).
[15] A. Rouzée, S. Guérin, O. Faucher, and B. Lavorel, Phys. Rev. A **77**, 043412 (2008).
[16] A. Rouzée, E. Hertz, B. Lavorel, and O. Faucher, J. Phys. B **41** (2008).
[17] S. S. Viftrup, V. Kumarappan, L. Holmegaard, C. Z. Bisgaard, H. Stapelfeldt, M. Artamonov, E. Hamilton, and T. Seideman, Phys. Rev. A **79**, 023404 (2009).
[18] H. Stapelfeldt and T. Seideman, Rev. Mod. Phys. **75**, 543 (2003).
[19] T. Seideman and E. Hamilton, Adv. At., Mol., Opt. Phys. **52**, 282 (2005).
[20] F. Filsinger, G. Meijer, J. Hansen, J. Maurer, J. Nielsen, L. Holmegaard, and H. Stapelfeldt, Angew. Chem. Int. Ed. **48**, 6900 (2009).
[21] E. Gershnabel and I. S. Averbukh, Phys. Rev. A **82**, 033401 (2010).
[22] E. Gershnabel and I. S. Averbukh, Phys. Rev. Lett. **104**, 153001 (2010).
[23] V. Loriot, E. Hertz, A. Rouzée, B. Sinardet, B. Lavorel, and O. Faucher, Opt. Lett. **31**, 2897 (2006).
[24] N. Kajumba, R. Torres, J. G. Underwood, J. S. Robinson, S. Baker, J. W.G. Tisch, R. d. Nalda, W. A. Bryan, R. Velotta, C. Altucci, I. Procino, I. C. E. Turcu, and J. P. Marangos, New J. Phys. **10**, 025008 (2008).
[25] X. Guo, P. Liu, Z. Zeng, P. Yu, R. Li, and N. Xu, Opt. Commun. **282**, 2539 (2009).
[26] L. Holmegaard, J. L. Hansen, L. Kalhoj, S. L. Kragh, H. Stapelfeldt, F. Filsinger, J. Küpper, G. Meijer, D. Dimitrovski, M. Abu-Samha, C. P. J. Martiny, and L. B. Madsen, Nat. Phys. **6**, 428 (2010).
[27] S. Pabst, P. J. Ho, and R. Santra, Phys. Rev. A **81**, 043425 (2010).
[28] S. Fleischer, I. S. Averbukh, and Y. Prior, Phys. Rev. Lett. **99**, 093002 (2007).
[29] S. Fleischer, I. S. Averbukh, and Y. Prior, J. Mod. Opt. **54**, 2641 (2007).
[30] S. Fleischer, I. S. Averbukh, and Y. Prior, J. Phys. B **41** (2008).
[31] E. Gershnabel and I. S. Averbukh, Phy. Rev. A **78**, 063416 (2008).
[32] Z. D. Sun, K. Takagi, and F. Matsushima, Science **310**, 1938 (2005).
[33] J. T. Hougen and T. Oka, Science **310**, 1913 (2005).
[34] H. C. Longuet-Higgins, Mol. Phys. **6**, 445 (1963).
[35] B. S. Ray, Z. Phys. **78**, 74 (1932).
[36] A. J. Russell and M. A. Spackman, Mol. Phys. **98**, 855 (2000).
[37] R. Tammer and W. Huttner, Mol. Phys. **83**, 579 (1994).
[38] M. J. Frisch, G. W. Trucks, H. B. Schlegel *et al.*, GAUSSIAN03, Gaussian, Inc., Pittsburgh, PA, 2004.
[39] H. W. Kroto, *Molecular rotation spectra*, reprint ed. (Dover, New York, 2003).
[40] R. N. Zare, *Angular momentum: Understanding spatial aspects in chemistry and physics* (Wiley, New York, 1988).
[41] S. C. Wang, Phys. Rev. **34**, 243 (1929).
[42] N. Moiseyev and T. Seideman, J. Phys. B **39**, L211 (2006).
[43] E. P. Wigner, *Group theory and its application to quantum theory* (Academic, New York, 1959).
[44] L. Ehn, I. Cernusak, and P. Neogrady, Croat. Chem. Acta **82**, 253 (2009).
[45] A. Pelzer, S. Ramakrishna, and T. Seideman, J. Chem. Phys. **129**, 134301 (2008).
[46] P. Felker, J. Phys. Chem. **96**, 7844 (1992).
[47] M. Leibscher, I. S. Averbukh, and H. Rabitz, Phys. Rev. A **69** (2004).
[48] S. Fleischer, I. S. Averbukh, and Y. Prior, Phys. Rev. A **74** (2006).
[49] S. Ramakrishna and T. Seideman, Phys. Rev. Lett. **99**, 103001 (2007).

[50]C. B. Madsen, L. B. Madsen, S. S. Viftrup, M. P. Johansson, T. B. Poulsen, L. Holmegaard, V. Kumarappan, K. A. Jørgensen, and H. Stapelfeldt, Phys. Rev. Lett. **102**, 073007 (2009).
[51]C. B. Madsen, L. B. Madsen, S. S. Viftrup, M. P. Johansson, T. B. Poulsen, L. Holmegaard, V. Kumarappan, K. A. Jorgensen, and H. Stapelfeldt, J. Chem. Phys. **130**, 234310 (2009).
[52]O. Deeb, M. Leibscher, J. Manz, W. v. Muellern, and T. Seideman, ChemPhysChem **8**, 322 (2007).
[53]T. Grohmann, O. Deeb, and M. Leibscher, Chem. Phys. **338**, 252 (2007).
[54]S. Belz, T. Grohmann, and M. Leibscher, J. Chem. Phys. **131**, 034305 (2009).
[55]T. Grohmann and M. Leibscher, J. Chem. Phys. **132**, 234301 (2010).
[56]P. R. Bunker, J. Mol. Spectrosc. **48**, 181 (1973).
[57]J. K. G. Watson, J. Mol. Spectrosc. **50**, 281 (1974).
[58]J. K. G. Watson, Can. J. Phys. **53**, 2210 (1975).